

## Synthesis, Characterization, and DNA Binding and Cleavage Properties of Copper(II)-tryptophanphenylalanine-1,10-phenanthroline/2,2'-bipyridine Complexes

by Pulimamidi R. Reddy\*, Nomula Raju, and Battu Satyanarayana

Department of Chemistry, Osmania University, Hyderabad – 500007, India  
(phone: +91-40-27171664; fax: +91-40-27090020; e-mail: rabi\_pr@rediffmail.com)

---

The mononuclear dipeptide-based Cu<sup>II</sup> complexes [Cu<sup>II</sup>(trp-phe)(phen)(H<sub>2</sub>O)]·ClO<sub>4</sub> (**1**) and [Cu<sup>II</sup>(trp-phe)(bpy)(H<sub>2</sub>O)]·ClO<sub>4</sub> (**2**) (trp-phe = tryptophanphenylalanine, phen = 1,10-phenanthroline, bpy = 2,2'-bipyridine) were isolated, and their interaction with DNA was studied. They exhibit intercalative mode of interaction with DNA. The intercalative interaction was quantified by Stern–Volmer quenching constant ( $K_{sv}$  = 0.14 for **1** and 0.08 for **2**). The Cu<sup>II</sup> complexes convert supercoiled plasmid DNA into its nicked circular form hydrolytically at physiological conditions at a concentration as low as 5 μM (for **1**) and 10 μM (for **2**). The DNA hydrolysis rates at a complex concentration of 50 μM were determined as 1.74 h<sup>-1</sup> ( $R$  = 0.985) for **1** and 0.65 h<sup>-1</sup> ( $R$  = 0.965) for **2**. The rate enhancement in the range of 2.40–4.10 × 10<sup>7</sup>-fold compared to non-catalyzed double-stranded DNA is significant. This was attributed to the presence of a H<sub>2</sub>O molecule in the axial position of the Cu complexes.

---

**Introduction.** – During the last decade, the interaction between transition metal complexes and DNA has received much attention [1–14], since binding studies of small molecules to DNA are important in the development of new therapeutic reagents and DNA probes [15–19]. Cu<sup>II</sup>–Peptide–diimine complexes were shown to bind to DNA in a nonspecific (noncovalent) mode of interaction such as electrostatic, groove [20][21], intercalative, and partial intercalative binding [22]. Synthesis, structure, and nuclease properties of ternary Cu<sup>II</sup>-peptides with 1,10-phenanthroline were reported and structurally characterized by X-ray crystallography [23]. Most of the applications of these complexes require that the complexes bind to DNA through an intercalative mode. Since aromatic moieties are known to play an important role in DNA binding through intercalation, we have isolated a peptide, trp-phe, with aromatic side chains and synthesized its Cu<sup>II</sup> complexes with phen and bpy ligands. The DNA-binding properties of these Cu<sup>II</sup> complexes were explored by spectroscopic and viscosity measurements. Their catalytic activity towards pUC19 DNA was also investigated. The rate of hydrolysis of DNA catalyzed by the complexes was determined by kinetics experiments. The rate enhancement in the range of 2.40–4.10 × 10<sup>7</sup>-fold compared to non-catalyzed double-stranded DNA is impressive.

**Results and Discussion.** – *Synthesis and Solubility.* The synthesis of **1** and **2** is schematically presented in *Scheme 1*. The complexes are partially soluble in MeOH and EtOH, but they show good solubility in aqueous MeOH/EtOH. They were non-



H<sub>2</sub>O), and the C=O band was shifted to 1654 cm<sup>-1</sup> upon complexation in both the complexes. The  $\nu_{as}$  (COO<sup>-</sup>) and  $\nu_s$  (COO<sup>-</sup>) stretching vibrations for **1** and **2** were observed at 1654 and 1384 cm<sup>-1</sup>, respectively. The large difference between the two values indicates that the COO<sup>-</sup> groups are coordinated to the metal ion in a monodentate fashion [24]. In phen, the peaks corresponding to the ring stretching frequencies ( $\nu$ (C=C) and  $\nu$ (C=N)) at 1502 and 1421 cm<sup>-1</sup> were shifted to higher frequencies (*ca.* 1518 and 1426 cm<sup>-1</sup>, resp.); in bpy, the peaks corresponding to the ring stretching frequencies ( $\nu$ (C=C) and  $\nu$ (C=N)) at 1557 and 1452 cm<sup>-1</sup> were shifted to 1603 and 1474 cm<sup>-1</sup>, respectively, indicating the coordination of the heterocyclic N-atoms to the Cu ion for **1** and **2**, respectively. The characteristic out-of-plane H-bending modes of free phen observed at 853 and 738 cm<sup>-1</sup> (for bpy at 780 and 714 cm<sup>-1</sup>) were shifted to 848 and 722 cm<sup>-1</sup> (for bpy 768 and 703 cm<sup>-1</sup>), respectively, upon metal complexation. The very strong bands at 1086 cm<sup>-1</sup> for **1** and 1094 cm<sup>-1</sup> for **2** were assigned to  $\nu$ (Cl–O) of ClO<sub>4</sub><sup>-</sup>. The rocking and wagging modes of M–OH<sub>2</sub> were observed at 920 cm<sup>-1</sup> and 623 cm<sup>-1</sup>, respectively, for both the complexes [25]. The new non-ligand peaks at 454 and 512 cm<sup>-1</sup> were assigned to  $\nu$ (Cu–O) and  $\nu$ (Cu–N) stretching vibrations, respectively [26]. These values are comparable with those observed for analogous Cu<sup>II</sup> complexes [23]. However, the slight variations may be attributed to the presence of an aromatic side chain in trp-phe.

The observed magnetic moment values ( $\mu_{\text{eff}} = 2.01$  and 1.69 BM for **1** and **2**, resp.) are indicative of paramagnetic nature of Cu complexes with spin (1/2) system [27].

The electronic spectra for the Cu<sup>II</sup> complexes were recorded in MeOH. Four absorption bands with varied intensity were observed for **1** (Fig. 1) and **2** (Fig. S1)<sup>1)</sup>. The intense bands at 206 and 222 nm of **1**, and 244 and 298 nm of **2** were assigned to intra-ligand ( $\pi$ – $\pi^*$ ) transition of phen and bpy ligands, respectively, while the less intense bands at 268 nm of **1** and at 310 nm of **2** were assigned to the LMCT transitions. Besides, a broad band observed at 626 nm for **1** and 613 nm for **2** in the spectra matches well with the reported  ${}^2B_{1g} \rightarrow {}^2B_{2g} - (\nu_1)$  ( $d_{x^2-y^2} \rightarrow d_{yz}$ ) transition of the five-coordinated Cu<sup>II</sup> in an approximate square-pyramidal geometry [28]. They agree well with the reported analogous systems [23].

The active chemical species of the complexes were identified by means of electrospray ionization mass spectrometry (ESI-MS). The peaks observed at *m/z* 593 and 587 were due to the formation of species [Cu(trp-phe)(phen)]<sup>+</sup> for **1** and [Cu(trp-phe)(bpy)]<sup>+</sup> + Na<sup>+</sup> for **2**.

The solid-state EPR spectra of **1** and **2** at room temperature was indicative of S = 1/2, which also showed four *g*-tensor *viz.*  $g_1$ ,  $g_2$ ,  $g_3$ , and  $g_4$  values at 2.04, 2.09, 2.17, and 2.45, respectively, for **1**, and 2.08, 2.15, 2.31, and 2.45, respectively for **2**, where  $g_4 > g_3 > g_2 > g_1$  (Table 2). It was observed earlier that if the value of  $g_4$  is higher than 2.3, it is indicative of covalent character of the M–L bonds [29].

The EPR spectra of the complexes provided good evidence for distinguishing the two ground states of five-coordinated structure, *i.e.*,  $d_{x^2-y^2}$  (square-pyramidal) and  $d_{z^2}$  (trigonal-bipyramidal). For the system with  $g_3 > g_2 > g_1$ , the ratio of  $(g_2 - g_1)/(g_3 - g_2)$ , hereafter called parameter *R*, will give information regarding the ground-state orbital. If  $R > 1$ , predominantly the ground-state is  $d_{z^2}$ , and if  $R < 1$ , the ground-state will

<sup>1)</sup> Supplementary material (Figs. S1–S4) for complex **2** is available upon request from the authors.

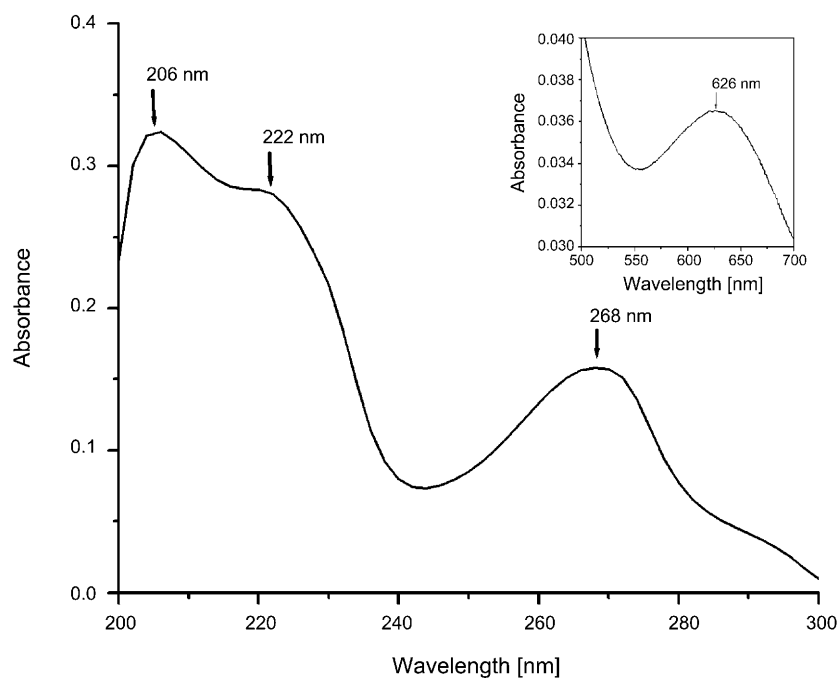


Fig. 1. UV/VIS Absorption spectra of complex **1** (inset: d → d transition).

Table 2. EPR Parameters of Complexes **1** and **2** (at room temperature)

Complex	$g_1$	$g_2$	$g_3$	$g_4$	$R^a$
$[\text{Cu}^{\text{II}}(\text{trp-phe})(\text{phen})(\text{H}_2\text{O})] \cdot \text{ClO}_4$ ( <b>1</b> )	2.04	2.09	2.17	2.45	0.625
$[\text{Cu}^{\text{II}}(\text{trp-phe})(\text{bpy})(\text{H}_2\text{O})] \cdot \text{ClO}_4$ ( <b>2</b> )	2.08	2.15	2.31	2.45	0.437

$$^a) R = (g_2 - g_1) / (g_3 - g_2).$$

be  $d_{x^2 - y^2}$ , which corresponds to square-pyramidal structure. The  $R$  ( $R < 1$ ) values for **1** and **2** (Table 2) indicate a  $d_{x^2 - y^2}$  ground state, which is consistent with a distorted square-pyramidal structure [30].

The thermal decomposition stoichiometries of the analytically characterized complexes were determined by TGA (thermogravimetric analyses). The spectra showed no mass loss in the temperature range of 25–180°. However, in the range of 180–240°, a mass loss of 3.2% (calc. 3.1%; 18 mass units) was observed. This is due to the loss of one coordinated  $\text{H}_2\text{O}$  molecule from **1** and **2**.

The minimum-energy conformers for the Cu complexes were calculated for the corresponding axial coordination of  $\text{H}_2\text{O}$  above and below the plane (Fig. 2 for **1**; Fig. S2, for **2**<sup>1</sup>). The energy differences between the two planes ( $\text{H}_2\text{O}$  coordination) were found to be 14.28 kcal/mol for **1** and 16.34 kcal/mol for **2**, respectively. The extra stability found in below-the-plane systems may be attributed to an intramolecular H-bonding network between the axial  $\text{H}_2\text{O}$  molecule and the C=O O-atom of  $\text{COO}^-$ , NH

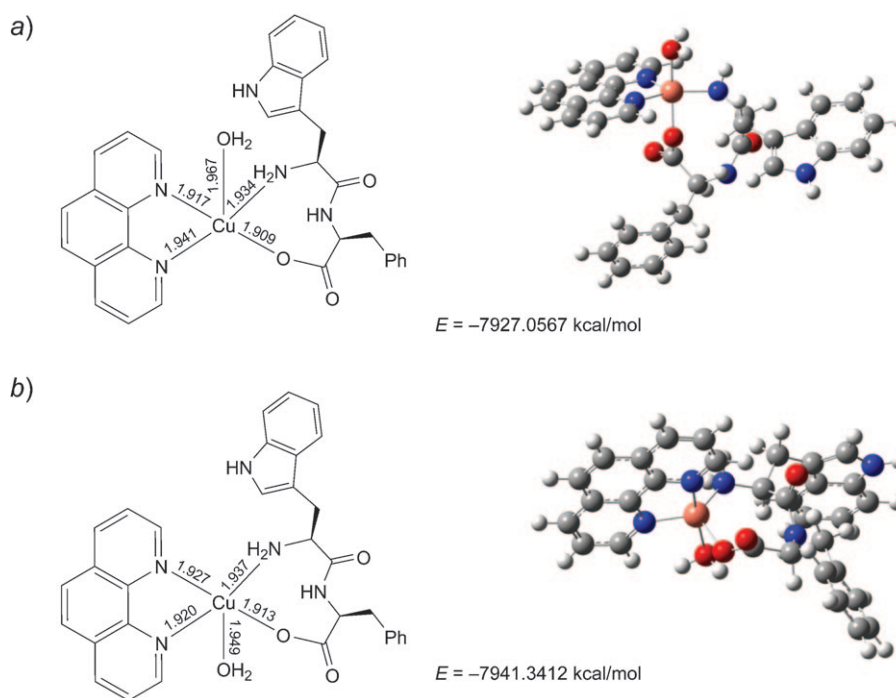


Fig. 2. Proposed geometry and energy-minimized molecular structures, relative energies, and bond lengths of **1** with  $H_2O$  molecule a) above and b) below the plane

of amide group, and the stacking interaction between the indole ring of peptide and phenyl ring of phen/bpy.

Based on the above results, a structure is proposed with an approximate square-pyramidal geometry where four equatorial positions are occupied by NN and NO donor atoms of phen/bpy and peptide, respectively, and the axial position is occupied by a  $H_2O$  molecule. This concurs with the X-ray structure of  $Cu^{II}$ -gly-trp-phen complex [23] where an amide N-atom was coordinated in the axial position instead of a  $H_2O$  molecule.

**DNA Binding.** The interaction of small molecules with double-helical DNA may increase or decrease  $T_m$ , the temperature at which the double helix is cleaved into a single-stranded DNA. While increase in  $T_m$  values indicates an intercalative or phosphate binding, decrease is typical for base binding. The thermal denaturation profile of DNA in the absence and presence of complexes is provided in Fig. 3. As can be seen, an increase of *ca.*  $4^\circ$  for **1** and *ca.*  $3^\circ$  for **2** was observed in the  $T_m$  profile of complexes as compared to free DNA. This provides a clear evidence for an intercalative/phosphate binding of Cu complexes with DNA.

Hydrodynamic measurements that are sensitive to length change (*i.e.*, viscosity and sedimentation) are regarded as the least ambiguous and the most critical tests of a binding model in solution in the absence of crystallographic structural data [31]. A classical intercalation model demands that the DNA helix must lengthen as base pairs

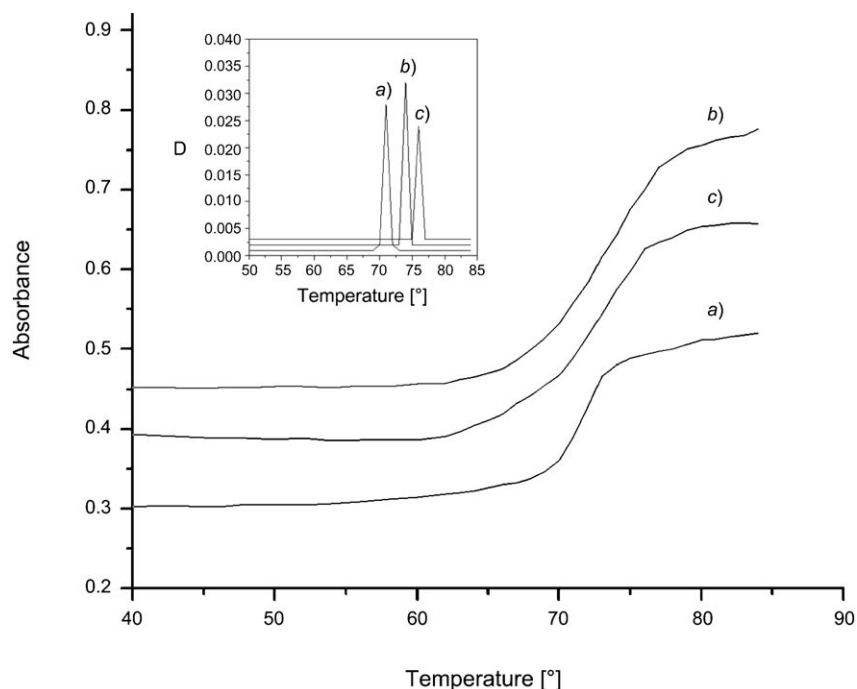


Fig. 3. Thermal denaturation profiles of a) free CT DNA, and b) and c) after addition of **1** and **2**, respectively. The concentrations of **1** or **2** and DNA were 30  $\mu\text{M}$ . Inset: differential melting curves.

are separated to accommodate the binding ligand/complex leading to an increase of DNA viscosity. In contrast, a partial intercalation of ligand/complex could bend (or kink) the DNA helix, and reduce its effective length and concomitantly its viscosity. The effect of **1** and **2** on the viscosity of DNA at room temperature is shown in Fig. 4. The viscosity of the DNA increases steadily with an increasing amounts of the complexes. Such behaviour is consistent with other intercalators (*i.e.*, EB), which increase the relative specific viscosity for the lengthening of the DNA double helix resulting from an intercalation. The results clearly emphasize that both of the complexes intercalate between adjacent DNA base pairs, causing an extension in the helix thereby increasing the viscosity of DNA [32].

Ethidium bromide (EB) emits intense fluorescence light in the presence of DNA, due to its strong intercalation between the adjacent DNA base pairs. It was reported earlier that the enhanced fluorescence can be quenched by the addition of a second molecule [33][34]. The extent of quenching fluorescence EB bound to DNA was used to determine the extent of binding between the second molecule and DNA. The emission spectra of EB bound to DNA in the absence and the presence of the complex **1** is shown in Fig. 5 (Fig. S3, for **2**<sup>1</sup>). The addition of complexes to DNA pretreated with EB caused appreciable reduction in emission intensity, indicating that the complexes efficiently compete with EB in binding to DNA. According to the Stern–Volmer equation,  $I_0/I = 1 + K_{sq}r$ , where  $I_0$  and  $I$  are the fluorescence intensities in

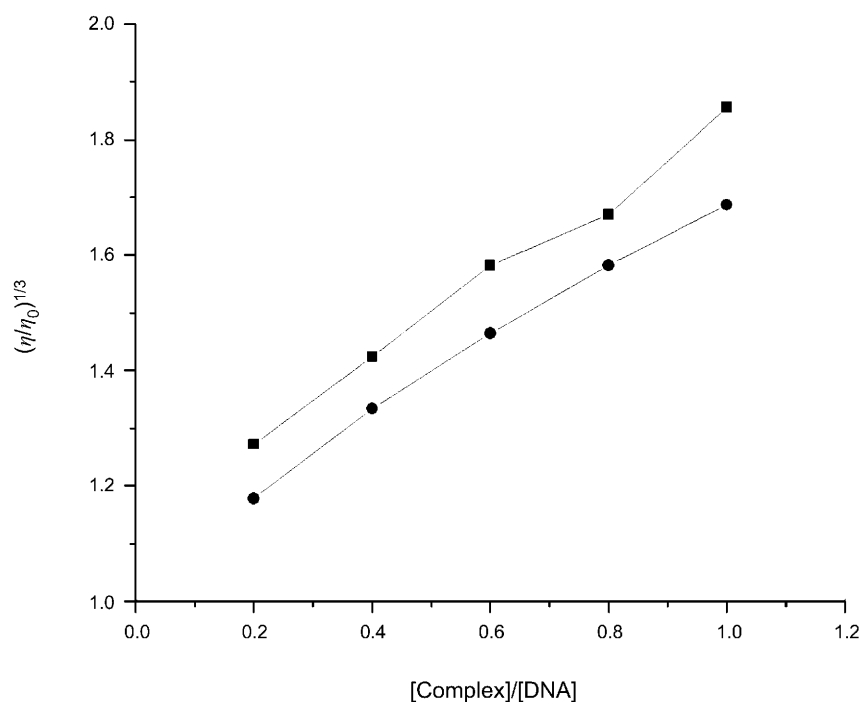


Fig. 4. Effect of increasing amounts of **1** (■) and **2** (●) on the relative viscosities of CT DNA at room temperature in 5 mM Tris · HCl buffer. Conditions: [DNA] = 200  $\mu$ M, [complex] = 0–200  $\mu$ M.

the absence and the presence of complexes, respectively,  $K_{sq}$  is linear *Stern–Volmer* quenching constant dependent on the ratio of concentration of bound EB to the concentration of DNA, and  $r$  is the concentration ratio of the complex to DNA. The quenching plots (Insets of Fig. 5 and Fig. S3<sup>1</sup>) illustrate that the quenching of EB bound to DNA by the complexes is in good agreement with the linear *Stern–Volmer* equation, which indicates that the complexes bind to DNA. In the plot of  $I_0/I$  vs. [complex]/[DNA],  $K_{sq}$  is given by the ratio slope/intercept, the  $K_{sq}$  values for **1** and **2** are 0.14 and 0.08, respectively.

Fluorescence *Scatchard* plots for the binding of EB to CT DNA in the presence of complexes were obtained as described by *Lepecq* and *Paoletti* [35]. The binding isotherms of EB and DNA in the absence and presence of the complexes were determined experimentally, and are presented in Fig. 6. As can be seen from the plots, a decrease of slope upon the addition of the complexes **1** and **2** confirm an exclusive intercalative mode of binding with DNA.

*DNA Cleavage.* The cleavage activity was demonstrated by gel-electrophoresis experiments using supercoiled (SC) plasmid pUC19 DNA in a medium Tris · HCl/NaCl buffer. These experiments were monitored by the addition of varying concentrations of the complex (0–100  $\mu$ M) to 2  $\mu$ l of pUC19 DNA, and the total volume was increased to 16  $\mu$ l by adding 5 mM Tris · HCl/5 mM NaCl buffer. When DNA was incubated with increasing concentrations of the complexes, SC DNA was degraded to nicked circular

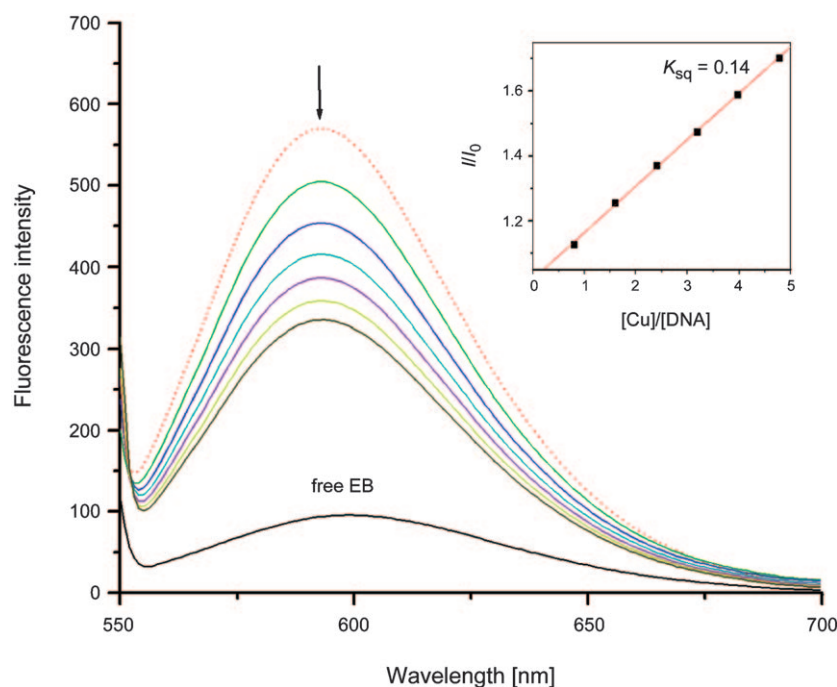


Fig. 5. Emission spectra of EB bound to DNA in the absence ( $\cdots$ ) and presence (—) of **1**.  $[1]/[DNA]=0, 0.8, 1.60, 2.41, 3.19, 3.97,$  and  $4.78, \lambda_{ex}=540$  nm. Inset: Stern–Volmer quenching plot.

(NC) form. The catalytic activities of **1** and **2** are depicted in Fig. 7. The activity of **1** starts at a concentration as low as  $5 \mu\text{M}$  (Fig. 7, a). At  $50 \mu\text{M}$ , a complete conversion of SC plasmid DNA into the NC form was observed, and at  $100 \mu\text{M}$  of **1**, the DNA was completely smeared (Fig. 7, b). In contrast, only 40% cleavage was achieved with **2** (Fig. 7, c). This may be due to the efficient binding of **1** with DNA compared to that of **2** and may also be due to the generation of stable  $[\text{Cu}(\text{phen})_2]^+$  species which could be related to the presence of an indole ring of trp-phe moiety, which is known to stabilize the radical species. Similar observations were made by García-Raso *et al.* [23].

To ensure that the Cu complexes are solely responsible for the cleavage, several control experiments were performed under identical conditions. No cleavage of DNA was observed with free Cu ( $100 \mu\text{M}$ ) and free ligands ( $100 \mu\text{M}$ ; Fig. 7, a; Lanes 5, 6, and 7, resp.). In a control experiment with DMSO ( $1 \text{ mM}$ ), a known radical scavenger, only slight inhibition (ca. 2%) of DNA cleavage was observed (Fig. 7, a, Lane 8 for **1**; and Fig. 7, c, Lane 7 for **2**), ruling out the possibility of DNA cleavage via  $\text{OH}^\cdot$ -based depurination pathway and also a possible oxidative cleavage [36] (dioxygen + Cu complex + traces of DNA). This observation indicates that the DNA cleavage was the result of hydrolysis of a phosphodiester bond [37–42]. Thus, the present study reveals that no diffusible radical is involved in the DNA cleavage, as no external agents like  $\text{H}_2\text{O}_2$ , MPA, ascorbic acid, or light were employed in the cleavage experiments.

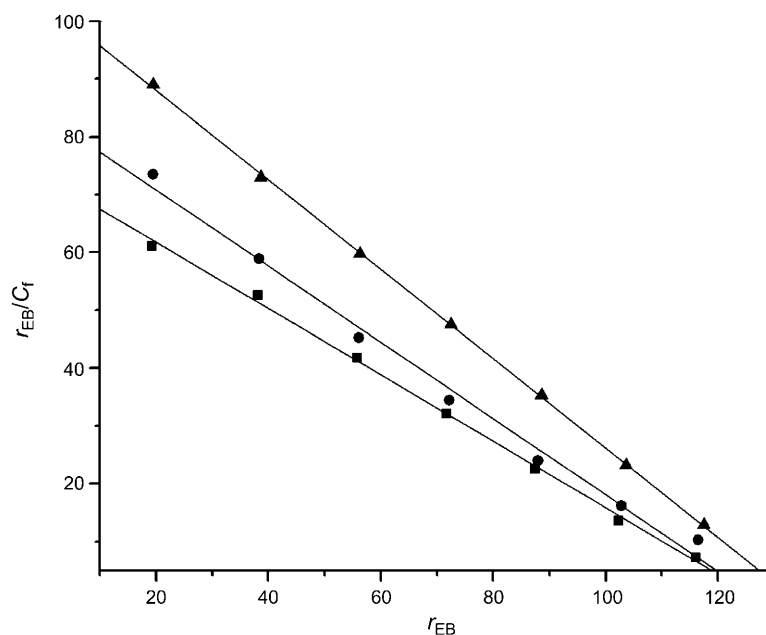


Fig. 6. Fluorescence Scatchard plots for the EB to CT DNA in the absence ( $\blacktriangle$ ) and presence of **1** ( $\blacksquare$ ) and **2** ( $\bullet$ ). The term  $r_{EB}$  is the concentration ratio of bound EB to total DNA, and  $c_f$  is the concentration of free EB.

The cleavage of pUC19 DNA by **1** and **2** was kinetically monitored by quantification of SC and NC forms of DNA. The observed distribution of SC and NC DNA in agarose gel provides a measure of the extent of hydrolysis of the phosphodiester bond in each plasmid DNA, and the data were used to perform simple kinetics. The kinetic plots (Fig. 8 for **1** and Fig. S4, for **2**), which show a decrease of SC and an increase of NC forms of DNA vs. time, follow the *pseudo*-first-order kinetics, and both forms fitted well to a single exponential curve. From these curve fits, the DNA hydrolysis rates were determined as  $1.74$  ( $R=0.985$ ) and  $0.65 \text{ h}^{-1}$  ( $R=0.963$ ) for **1** and **2**, respectively. The enhancement of DNA hydrolysis rate constant by metal complexes in the range of  $0.09\text{--}0.25 \text{ h}^{-1}$  was considered impressive [43][44]. With the rate constants of  $1.74$  (for **1**) and  $0.65 \text{ h}^{-1}$  (for **2**), which amounts to  $2.40\text{--}4.10 \times 10^7$ -fold rate enhancement compared to non-catalysed double stranded DNA, is significant considering the type of ligands and experimental conditions.

Based on the above conclusions, a tentative mechanism for the hydrolytic cleavage of DNA may be as follows: *i*) activation of the Cu-coordinated  $\text{H}_2\text{O}$  molecule, and formation of a nucleophile Cu–OH species; *ii*) phosphodiester coordination with amide and amine N-atoms through an electrostatic interaction; *iii*) intramolecular OH transfer from  $\text{Cu}^{\text{II}}$  to phosphate. There are literature reports on an intramolecular pathway for the hydrolysis of phosphate diester [45]. A hydrolytic cleavage mechanism was established by enzymatic religation of the termini with T4 DNA ligase which

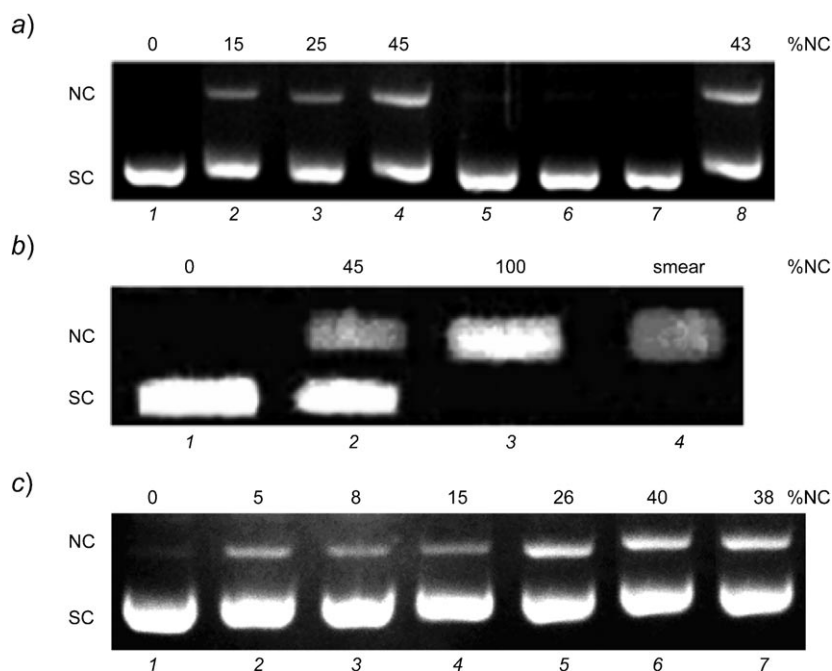


Fig. 7. Agarose gel-electrophoresis pattern for the cleavage of supercoiled pUC19 DNA by **1** and **2** at 37° in a buffer containing 5 mM Tris·HCl/5 mM aqueous NaCl. a) Lane 1: DNA control, Lane 2: DNA + **1** (5 μM), Lane 3: DNA + **1** (10 μM), Lane 4: DNA + **1** (25 μM), Lane 5: DNA + Cu(NO<sub>3</sub>)<sub>2</sub> (100 μM), Lane 6: DNA + phen (100 μM), Lane 7: DNA + trp-phen (100 μM), Lane 8: DNA + **1** (25 μM) + DMSO (1 mM). b) Lane 1: DNA control, Lane 2: DNA + **1** (25 μM), Lane 3: DNA + **1** (50 μM), Lane 4: DNA + **1** (100 μM). c) Lane 1: DNA control, Lane 2: DNA + **2** (10 μM), Lane 3: DNA + **2** (25 μM), Lane 4: DNA + **2** (50 μM), Lane 5: DNA + **2** (75 μM), Lane 6: DNA + **2** (100 μM), Lane 7: DNA + **2** (100 μM) + DMSO (1 mM).

requires 5'-phosphate and 3'-OH groups. Based on the efficiency of religation, it was concluded that hydrolysis gave equally probable 3'- and 5'-products [46].

Accordingly, a L–M–OH form, which is the active species in the hydrolysis of phosphate backbone in an enzyme/model, is depicted in *Scheme 2*.

**Conclusions.** – Two new Cu<sup>II</sup>–peptide–phen/bpy complexes were successfully synthesized, and their structures were established. Their DNA binding and cleavage abilities were investigated. The Cu<sup>II</sup> complexes bind to CT DNA in an exclusive intercalative mode. They show good catalytic activity in the absence of any external agents or light under physiological conditions.

*P. R. R.* thanks the *Council of Scientific and Industrial Research (CSIR)* New Delhi for financial assistance through major research project. He also thanks *UGC* for the award of *Emeritus Fellowship*.

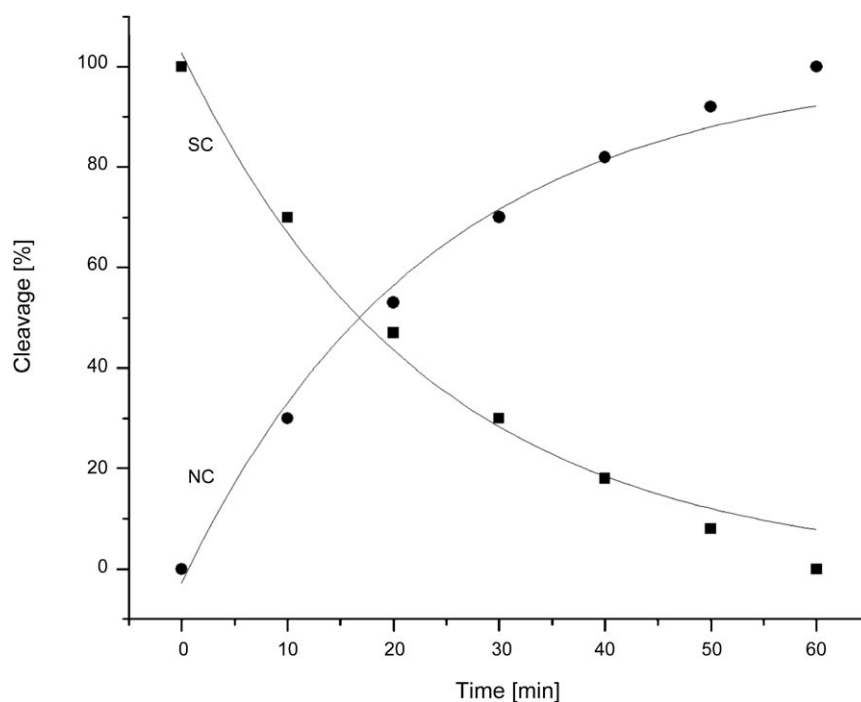
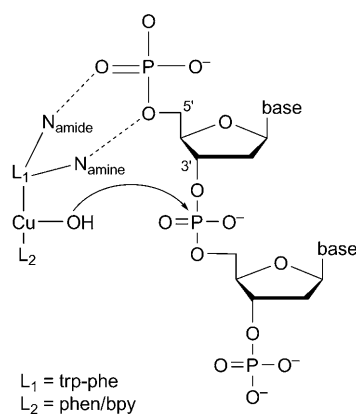


Fig. 8. Disappearance of supercoiled (SC) DNA and formation of nicked circular form (NC) in the presence of complex **1**. Conditions: [complex] = 50  $\mu$ M; in aqueous buffer (pH 7.2) at 37 $^{\circ}$ .

Scheme 2. A Proposed Mechanism for the DNA Cleavage



**Experimental Part**

*General.* Boc-tryptophan, phenylalanine methyl ester,  $\text{Cu}(\text{NO}_3)_2 \cdot 3 \text{H}_2\text{O}$ , 2,2'-bipyridine, 1,10-phenanthroline, and ethidium bromide (EB) were obtained from *Sigma* (99.99% purity), USA, and were of anal. grade. The peptide trp-phe was synthesized by the known procedure [47]. The calf thymus

(CT) DNA was obtained from *Fluka* (Switzerland); and pUC 19 DNA, agarose, and *Tris*·HCl were obtained from *Bangalore Genei* (India). All the chemicals were used as supplied. UV/VIS Spectra: *Shimadzu 160A* spectrophotometer (800–200 nm) and *JASCO V-530* UV/VIS spectrophotometer; with 1-cm quartz micro-cuvettes. IR Spectra: *Perkin-Elmer* FT-IR spectrometer, in KBr pellets, in the 4000–400  $\text{cm}^{-1}$  range. ESI-MS: *Quattro Lc* (*Micro mass*, Manchester, UK) triple quadrupole mass spectrometer with *MassLynx* software. Elemental analyses: *Heraeus Carlo Erba 1108* elemental analyzer. Molar conductivity: *Digisun* digital conductivity bridge (model: *DI-909*) with a dip-type cell. Magnetic susceptibilities of complexes: at r.t. on a *Faraday* balance (*CAHN-7600*) using  $\text{Hg}[\text{Co}(\text{NCS})_4]$  as the standard; diamagnetic corrections were made by using *Pascal's* constants [48]. EPR Spectra: *JEOL (JES-FA200)* X-band spectrometer at r.t. TGA Analyses: *METTLER TOLEDO (TGA/SDTA 851e)* thermo-analyzer at 25–300°, heating rate of 5°/min. The molecular-modeling calculations were carried out with semi-empirical PM3 Hamiltonian as implemented in *hyperchem* software programme package. Gel pattern of electrophoresis was photographed by *Alpha-Innotec* gel documentation system (USA).

Concentrated CT DNA stock soln. was prepared in 5 mM *Tris*·HCl/50 mM NaCl in double dist.  $\text{H}_2\text{O}$  at pH 7.5, and the concentration of DNA soln. was determined by UV absorbance at 260 nm ( $\epsilon = 6600 \text{ M}^{-1} \text{ cm}^{-1}$ ) [49]. Soln. of CT DNA in 5 mM *Tris*·HCl/50 mM NaCl (pH 7.5) gave a ratio of UV absorption at 260 and 280 nm,  $A_{260}/A_{280}$ , of ca. 1.8–1.9, indicating that the DNA was sufficiently free of protein [50]. All stock solns. were stored at 4° and were used within 4 d. The concentration of EB was determined spectrophotometrically at 480 nm ( $\epsilon = 5680 \text{ M}^{-1} \text{ cm}^{-1}$ ) [51].

*Syntheses of Peptide and Complexes.* The dipeptide trp-phe was synthesized by conventional soln.-phase method [47] using EDCI and HOBt as coupling agents and dry  $\text{CH}_2\text{Cl}_2$  as solvent. While (*tert*-butoxy)carbonyl (Boc) group was used for N-protection, the C-terminal was protected as methyl ester (COOMe). Deprotection of Boc was achieved with TFA/ $\text{CH}_2\text{Cl}_2$  1:1, and saponification of the methyl ester required LiOH in THF/MeOH/ $\text{H}_2\text{O}$  3:1:1.  $^1\text{H-NMR}$  (200 MHz,  $\text{CDCl}_3$ ): 2.00 (br., 2 H); 2.93–3.95 (m, 5 H); 4.85 (m, 1 H); 6.82–7.20 (m, 8 H); 7.21 (m, 2 H); 8.00 (m, 1 H); 10.10 (d, 2 H). ESI-MS: 351.

To a mixture of trp-phe (0.351 g, 1.0 mmol) and KOH (0.056 g, 1.0 mmol) in  $\text{H}_2\text{O}$ , an aq. soln. of  $\text{Cu}(\text{NO}_3)_2 \cdot 3 \text{H}_2\text{O}$  (0.241 g, 1.0 mmol) was added with stirring, followed by the addition of phen (0.198 g, 1.0 mmol) or bpy soln. (0.156 g, 1.0 mmol) in MeOH (2 ml). The stirring was continued for ca. 3 h at 60°. After cooling to r.t., an aq. soln. of  $\text{NaClO}_4 \cdot \text{H}_2\text{O}$  (0.181 g, 1.0 mmol) was added, and stirring was continued for another 30 min. The resulting violet-blue precipitate was filtered and washed with EtOH and cyclohexane, and dried *in vacuo* to afford 72 and 65% of **1** and **2**, resp.

*Data of  $[\text{Cu}^{\text{II}}(\text{trp-phe})(\text{phen})(\text{H}_2\text{O})]\text{ClO}_4$  (**1**).* UV/VIS (MeOH): 626, 268, 222, 206. IR (KBr): 3420 (br.), 3263s, 2953m, 1684vs, 1654s, 1576m, 1518s, 1426s, 1384s, 1146m, 1086m, 920m, 848s, 722m, 623w, 512m, 454m. ESI-MS: 593 ( $[\text{Cu}(\text{trp-phe})(\text{phen})]^+$ ). Anal. calc. for  $\text{C}_{32}\text{H}_{30}\text{ClCuN}_5\text{O}_8$  (711.61): C 54.01, H 4.25, N 9.84; found: C 53.01, H 4.02, N 9.95.  $\mu_{\text{eff}} = 2.01$  BM.  $A_{\text{M}}$  ( $10^{-3}$  M in MeOH, 25°) =  $1.60 \Omega^{-1} \text{ cm}^2 \text{ mol}^{-1}$ .

*Data of  $[\text{Cu}^{\text{II}}(\text{trp-phe})(\text{bpy})(\text{H}_2\text{O})]\text{ClO}_4$  (**2**).* UV/VIS (MeOH): 613, 310, 298, 244. IR (KBr): 3446 (br.), 3253s, 2954m, 1684vs, 1654s, 1603m, 1474s, 1445vs, 1382s, 1250m, 1094m, 1032s, 768vs, 731m, 703m, 623w, 512m, 454m. ESI-MS: 587 ( $[[\text{Cu}(\text{trp-phe})(\text{bpy})] + \text{Na}]^+$ ). Anal. calc. for  $\text{C}_{30}\text{H}_{30}\text{ClCuN}_5\text{O}_8$  (687.59): C 52.40, H 4.40, N 10.19; found: C 52.01, H 4.25, N 10.56.  $\mu_{\text{eff}} = 1.69$  BM.  $A_{\text{M}}$  ( $10^{-3}$  M in MeOH, 25°) =  $2.10 \Omega^{-1} \text{ cm}^2 \text{ mol}^{-1}$ .

*DNA Binding. Thermal-Denaturation Studies.* The thermal-denaturation studies were performed on *Shimadzu 160A* spectrophotometer equipped with a thermostatic cell holder. DNA (30  $\mu\text{M}$ ) was treated with complexes **1** or **2** (30  $\mu\text{M}$ ) in a ratio of 1:1 in buffer (5 mM *Tris*·HCl/50 mM NaCl) at pH 7.5. The samples were continuously heated at the rate of 1°/min while monitoring the absorption changes at 260 nm. Melting-temp. ( $T_{\text{m}}$ ) and the melting-interval ( $\Delta T_{\text{m}}$ ) data were obtained according the procedure reported in [52].

*Viscometric Studies.* Viscometric titrations were performed with an *Ostwald* viscometer at r.t. The concentration of DNA was 200  $\mu\text{M}$ , complex concentration was varied from 0–200  $\mu\text{M}$ , and the flow times were measured with a digital timer. Each sample was measured three times for accuracy, and an average flow time was determined. Data is presented as  $(\eta/\eta_0)^{1/3}$  vs.  $[\text{complex}]/[\text{DNA}]$ , where  $\eta$  is the viscosity of DNA in the presence of complex and  $\eta_0$  that of DNA alone. Viscosity values were calculated from the

observed flow time of DNA containing solns. ( $t$ ) corrected for that buffer alone (5 mM *Tris*·HCl/50 mM NaCl) ( $t_0$ ),  $\eta = (t - t_0)$ .

**Fluorescence-Spectroscopic Studies.** Fluorescence spectra were recorded with *SPEX-Fluorolog* 0.22 m fluorimeter equipped with a 450-W Xe lamp. The slit widths were  $2 \times 2 \times 2$ , and the emission spectral range was 550–650 nm. All fluorescence titrations were carried out in 5 mM *Tris*·HCl/50 mM NaCl (pH 7.5). Soln. containing DNA and EB was titrated with varying concentrations of **1** and **2**. The concentration of DNA and EB was maintained at 41  $\mu$ M, and the concentration of complexes was in the range of 0–196  $\mu$ M. The solns. containing DNA and EB were mixed (equimolar ratio), and the complexes **1** and **2** were added and allowed to equilibrate. They were excited at 540 nm ( $\lambda_{\text{max}}$  for EB), and the fluorescence emissions at 598 nm ( $\lambda_{\text{max}}$ ) were recorded.

Fluorescence spectra were also utilized to obtain *Scatchard* plots. For this, titration of DNA against EB in the absence and presence of Cu complexes were performed. Initial concentration of DNA in 5 mM *Tris*·HCl/50 mM NaCl was 20  $\mu$ M, and the concentration of **1** and **2** were kept at 50  $\mu$ M. After each addition of EB to the solns. containing DNA and Cu complexes, the emission spectra were recorded in the range of 550–650 nm with excitation at 540 nm at 25°. Corrections were made to the data for the volume changes during the course of titrations. The data were analyzed by the method of *Lepecq* and *Paoletti* [35] to obtain bound ( $c_b$ ) and free ( $c_f$ ) concentration of EB, and *Scatchard* plots were obtained by plotting  $r_{\text{EB}}/c_f$  vs.  $r_{\text{EB}}$  (where  $r = c_b/\text{conc. of DNA}$ ).

**DNA Cleavage.** The DNA cleavage experiments were performed with supercoiled (SC) plasmid pUC19 DNA at pH 7.2 in *Tris*·HCl buffer. DNA Cleavage experiments were monitored by the addition of varying concentrations of the complexes **1** and **2** (0–100  $\mu$ M) to 2  $\mu$ l of pUC19 DNA, the total volume was increased to 16  $\mu$ l by adding 5 mM *Tris*·HCl/5 mM NaCl buffer. After mixing, DNA solns. were incubated for 1 h at 37°. The samples were subjected to electrophoresis in TAE (*Tris*·AcOH EDTA buffer) for 2 h at 60 V. The gel was stained with 0.5  $\mu$ g/ml EB and photographed under UV light.

Blank experiments were carried out using free  $\text{Cu}(\text{NO}_3)_2 \cdot 3 \text{H}_2\text{O}$  and free ligands (trp-phe, phen) at 100  $\mu$ M. Experiments were also carried out with known radical scavenger DMSO. Kinetic analyses were carried out at a fixed concentration of DNA and **1** or **2** (50  $\mu$ M), with different incubation times under identical experimental conditions.

#### REFERENCES

- [1] M. J. Clarke, F. Zhu, D. R. Frasca, *Chem. Rev.* **1999**, *99*, 2511.
- [2] J. Liu, W.-J. Mei, A.-W. Xu, C.-P. Tan, S. Shi, L.-N. Ji, *Antiviral Res.* **2004**, *66*, 65.
- [3] J. Liu, W.-J. Mei, A.-W. Xu, C.-P. Tan, L.-N. Ji, *Transition Met. Chem. (Dordrecht, Neth.)* **2003**, *28*, 500.
- [4] D. S. Sigman, A. Mazumder, D. M. Perrin, *Chem. Rev.* **1993**, *93*, 2295.
- [5] K. E. Erkkila, D. T. Odom, J. K. Barton, *Chem. Rev.* **1999**, *99*, 2777.
- [6] M. Narra, P. Elliott, S. Swavey, *Inorg. Chim. Acta* **2006**, *359*, 2256.
- [7] D. Lawrence, V. G. Vaidyanathan, B. U. Nair, *J. Inorg. Biochem.* **2006**, *100*, 1244.
- [8] H. Chao, L.-N. Ji, *Bioinorg. Chem. Appl.* **2005**, *3*, 15.
- [9] L.-F. Tan, H. Chao, Y.-J. Liu, H. Li, B. Sun, L.-N. Ji, *Inorg. Chim. Acta* **2005**, *358*, 2191.
- [10] J.-Z. Wu, L. Yuan, Y. Yu, *Inorg. Chim. Acta* **2006**, *359*, 718.
- [11] A. E. Friedman, J. C. Chambron, J. P. Sauvage, N. J. Turro, J. K. Barton, *J. Am. Chem. Soc.* **1990**, *112*, 4960.
- [12] L.-F. Tan, H. Chao, H. Li, Y.-J. Liu, B. Sun, W. Wei, L.-N. Ji, *J. Inorg. Biochem.* **2005**, *99*, 513.
- [13] P. J. Dandliker, R. E. Holmlin, J. K. Barton, *Science* **1997**, *275*, 1465.
- [14] I. Ortmans, C. Moucheron, A. Kirsch-De Mesmaeker, *Coord. Chem. Rev.* **1998**, *168*, 233.
- [15] L.-N. Ji, X.-H. Zou, J.-G. Liu, *Coord. Chem. Rev.* **2001**, *216–217*, 513.
- [16] H. Xu, K.-C. Zheng, L.-J. Lin, H. Li, Y. Gao, L.-N. Ji, *J. Inorg. Biochem.* **2004**, *98*, 87.
- [17] Y.-J. Liu, H. Chao, L.-F. Tan, Y.-X. Yuan, W. Wei, L.-N. Ji, *J. Inorg. Biochem.* **2005**, *99*, 530.
- [18] G. Yang, J. Z. Wu, L. Wang, L. N. Ji, X. Tian, *J. Inorg. Biochem.* **1997**, *66*, 141.
- [19] G. Yang, L. Wang, L.-N. Ji, *J. Inorg. Biochem.* **1997**, *67*, 289.

- [20] Y. Jin, M. A. Lewis, N. H. Gokhale, E. C. Long, J. A. Cowan, *J. Am. Chem. Soc.* **2007**, *129*, 8353.
- [21] R. Nagane, T. Koshigoe, M. Chikira, E. C. Long, *J. Inorg. Biochem.* **2001**, *83*, 17.
- [22] R. S. Kumar, S. Arunachalam, *Eur. J. Med. Chem.* **2009**, *44*, 1878.
- [23] Á. García-Raso, J. J. Fiol, B. Adrover, V. Moreno, I. Mata, E. Espinosa, E. Molins, *J. Inorg. Biochem.* **2003**, *95*, 77.
- [24] L. H. Abdel-Rehman, L. P. Battaglia, M. R. Mahmoud, *Polyhedron* **1996**, *15*, 327.
- [25] K. Nakamoto, 'Infrared and Raman Spectra of Inorganic and Coordination Compounds', 3rd edn., John Wiley & Sons, New York, p. 228.
- [26] G. G. Mohamed, M. M. Omar, A. M. M. Hindy, *Spectrochim. Acta, Part A* **2005**, *62*, 1140.
- [27] R. N. Patel, N. Singh, V. L. N. Gundla, *Indian J. Chem., Sect. A* **2006**, *45*, 614.
- [28] T. Murakami, S. Hatakeyama, S. Igarashi, Y. Yukawa, *Inorg. Chim. Acta* **2000**, *310*, 96.
- [29] D. Kivelson, R. Neiman, *J. Chem. Phys.* **1961**, *35*, 149.
- [30] P. Kopel, Z. Trávníček, J. Marek, M. Korabik, J. Mrozinski, *Polyhedron* **2003**, *22*, 411.
- [31] S. Satyanarayana, J. C. Dabrowiak, J. B. Chaires, *Biochemistry* **1993**, *32*, 2573.
- [32] S. Satyanarayana, J. C. Dabrowiak, J. B. Chaires, *Biochemistry* **1992**, *31*, 9319.
- [33] B. C. Baguley, M. Le Bret, *Biochemistry* **1984**, *23*, 937.
- [34] J. R. Lakowicz, G. Webber, *Biochemistry* **1973**, *12*, 4161.
- [35] J.-B. Lepecq, C. Paoletti, *J. Mol. Biol.* **1967**, *27*, 87.
- [36] R. Ren, P. Yang, W. Zheng, Z. Hua, *Inorg. Chem.* **2000**, *39*, 5454.
- [37] L. A. Basile, A. L. Raphael, J. K. Barton, *J. Am. Chem. Soc.* **1987**, *109*, 7550.
- [38] T. Itoh, H. Hisada, T. Sumiya, M. Hosono, Y. Usui, Y. Fujii, *Chem. Commun.* **1997**, 677.
- [39] K. M. Deck, T. A. Tseng, J. N. Burstyn, *Inorg. Chem.* **2002**, *41*, 669.
- [40] L. Zhu, O. dos Santos, C. W. Koo, M. Rybstein, L. Pape, J. W. Canary, *Inorg. Chem.* **2003**, *42*, 7912.
- [41] L. Bonfá, M. Gatos, F. Mancin, P. Tecilla, U. Tonellato, *Inorg. Chem.* **2003**, *42*, 3943.
- [42] F. Mancin, P. Tecilla, *New J. Chem.* **2007**, *31*, 800.
- [43] J. Rammo, R. Hettich, A. Roigk, H.-J. Schneider, *Chem. Commun.* **1996**, 105.
- [44] A. Roigk, R. Hettich, H.-J. Schneider, *Inorg. Chem.* **1998**, *37*, 751.
- [45] J.-H. Li, J.-T. Wang, P. Hu, L.-Y. Zhang, Z.-N. Chen, Z.-W. Mao, L.-N. Ji, *Polyhedron* **2008**, *27*, 1898.
- [46] R. Ott, R. Krämer, *Appl. Microbiol. Biotechnol.* **1999**, *52*, 761.
- [47] M. Bodanszky, A. Bodanszky, 'The Practices of Peptide Synthesis', Springer, New York, 1984.
- [48] B. N. Figgis, J. Lewis, 'Modern Coordination Chemistry', Eds. J. Lewis, R. C. Wilkinson, Wiley Interscience, New York, 1967, pp. 403.
- [49] J. Marmur, *J. Mol. Biol.* **1961**, *3*, 208.
- [50] M. E. Reichmann, C. A. Rice, C. A. Thomas, P. Doty, *J. Am. Chem. Soc.* **1954**, *76*, 3047.
- [51] F. Garland, D. E. Graves, L. W. Yielding, H. C. Cheung, *Biochemistry* **1980**, *19*, 3221.
- [52] 'Methods in Molecular Biology', Eds. W. D. Wilson, F. A. Tanious, M. Fernandez-Saiz, C. T. Rigl, K. R. Fox, Humana, Clifton, New Jersey, 1997, pp. 90.

Received November 21, 2010